JCTC Journal of Chemical Theory and Computation

Article

pubs.acs.org/JCTC

SplitGAS Method for Strong Correlation and the Challenging Case of Cr_2

Giovanni Li Manni,*[,†,‡] Dongxia Ma,[†] Francesco Aquilante,[‡,§,∥] Jeppe Olsen,[⊥] and Laura Gagliardi*[,†]

[†]Department of Chemistry, Supercomputing Institute, and Chemical Theory Center, University of Minnesota, Minneapolis, Minnesota 55455, United States

[‡]Department of Physical Chemistry, University of Geneva, Switzerland, CH-1211

[§]Center for Biomolecular Nanotechnologies @UNILE, Italian Institute of Technology (IIT), Via Barsanti, I-73010 Arnesano (LE), Italy

[∥]Department of Chemistry - Ångström, The Theoretical Chemistry Programme, Uppsala University, P.O. Box 518, SE-751 20 Uppsala, Sweden

[⊥]Department of Chemistry, Aarhus University, Langelandsgade 140, 8000 Aarhus C, Denmark

Supporting Information

ABSTRACT: A new multiconfigurational quantum chemical method, SplitGAS, is presented. The configuration interaction expansion, generated from a generalized active space, GAS, wave function is split in two parts, a principal part containing the most relevant configurations and an extended part containing less relevant, but not negligible, configurations. The partition is based on an orbital criterion. The SplitGAS method has been employed to study the HF, N_2, and Cr_2 molecules. The results on these systems, especially on the challenging, multiconfigurational Cr_2 molecule, are satisfactory. While SplitGAS is comparable with the GASSCF method in terms of memory requirements, it performs better than the complete active space method followed by second-order perturbation theory, CASPT2, in terms of equilibrium bond length, dissociation energy, and vibrational properties.

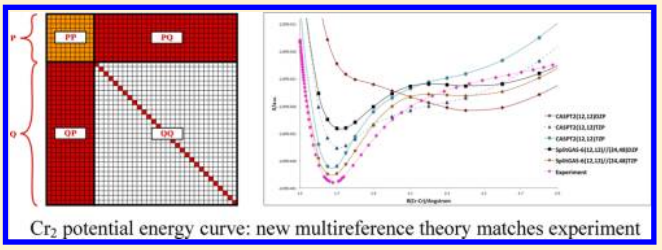

Cr_2 potential energy curve: new multireference theory matches experiment

I. INTRODUCTION

Chemical systems with a multiconfigurational electronic structure in their ground state and/or excited states are important in a number of contexts. For example, such systems can be precursors of novel materials with unusual spin properties[1−3] or have interesting catalytic applications.[4−7] However, such strongly correlated systems represent a challenge for modern quantum chemistry. Quantum chemical methods based on a single electronic configuration cannot correctly describe these systems, and multireference methods are instead required. A qualitative description of a strongly correlated system is provided by the Complete Active Space Self-Consistent Field (CASSCF) method,[8] where the orbital optimization is performed for a Full Configuration Interaction (FCI) including the strongly correlated orbitals as active orbitals. Currently, the size limit of CASSCF calculations is about 18 electrons in 18 orbitals (singlet spin state). This limit is due to the exponential scaling of the FCI expansion as a function of the number of the active orbitals and electrons. Therefore, even significant progress in computer technology will not make a tangible difference in the size of accessible active spaces.

The second-order complete active space perturbation method, CASPT2,[9] is an efficient method to describe dynamic correlation for strongly correlated systems, and this method has been extensively and successfully applied for a large number of challenging systems. There are a number of drawbacks and limitations of the CASPT2 method. These include (i) the limitation in the size of the reference complete active space (CAS) wave function; (ii) the intruder state problem contaminating the first-order wave function correction which can be partially solved by a level-shift correction (LS-CASPT2);[10,11] (iii) the overestimation of the energy of high-multiplicity states which requires the IPEA zeroth-order Hamiltonian;[12] (iv) the lack of orthogonality of the individual single-state CASPT2 solutions, which was solved by developing the multistate (MS) CASPT2 approach.[13,14]

The implementation of the Cholesky decomposition (CD) approach in the CASPT2 method[15−17] has extended its applicability to larger basis sets and thereby larger molecular systems. For instance, a 1000 basis set CD-CASPT2 calculation is feasible nowadays within the MOLCAS package.[18] Truncation of the virtual space in CD-CASPT2 calculations is also possible.[19] However, the CD does not reduce the complexity of the underlying FCI expansion, so there are many quantum-chemical systems for which CASPT2 cannot provide an accurate result. The implementation of the second-

Received: January 18, 2013

   dx.doi.org/10.1021/ct400046n | J. Chem. Theory Comput. XXXX, XXX, XXX−XXX

order perturbation theory restricted active space (RASPT2) method allows the use of larger active spaces and extends therefore the range of applicability of multireference second-order perturbation methods.[20−23] This development has been followed by the formulation of the Generalized Active Space (GAS) method.[24] In GAS the user has the possibility of choosing an arbitrary number of active spaces and control the interspace excitations by means of constraints on the occupation number of such spaces.

With the aim at approximating CASSCF wave functions, density matrix renormalization group (DMRG) algorithms[25−28] can potentially treat active spaces much beyond the nominal limit (18 electrons in 18 orbitals). Although DMRG matrix product states are often referred to as reproducing the corresponding CASSCF wave functions, the underlying polynomial parametrization is not guaranteed to account for all electron correlation effects included in the FCI ansatz. Despite this fundamental difference, DMRG algorithms provide CASSCF-quality reference functions for PT2 correlation treatment, as demonstrated by a recent study on the challenging electronic structure of the chromium dimer.[29]

We have recently formulated the SplitCAS approach.[30] The basic idea is to partition the CI-expansion generated from a CAS expansion into two parts, a principal part (P) containing the most relevant configurations and an extended part (Q) containing less relevant (but not negligible) configurations. The CI-Hamiltonian matrix is partitioned into four blocks accordingly. By using Löwdin's partitioning technique[31] and a diagonal approximation for the interaction between two states in the (Q) space, it is possible to reduce the full matrix problem to an effective matrix problem of the size of the principal block (PP). The principal block is thus dressed perturbatively through the extended blocks and then diagonalized. The key-point of these Split-type methods is the criteria chosen for the splitting between the (P) and the (Q) space. In our original work[30] we proposed an energy-based splitting. The Configuration State Functions, CSFs, are first generated, then ordered according to their energy, and finally divided into (P) and (Q) parts, according to a user specific energetic threshold. This energy-based variant of the SplitCAS approach has similarities with later modifications of Löwdin's partitioning technique like Davidson's "Reduced Model Space" approach[32,33] and Shavitt's "B_k" method.[34] These techniques encounter complications from an algorithmic point of view, because they are not compatible with standard Direct CI implementations requiring expansions defined by occupations in one or several orbital-subspaces. At this stage we should also mention, as an approach to the electron correlation problem, the multireference, state-specific, second-order, Brillouin−Wigner perturbation theory[35,36] and the active-space reduced density matrix method.[37]

In this paper, we report the formulation and implementation of a Split-type method based on an orbital partitioning. We refer to this method as SplitGAS, because it is based on a GASSCF-type of wave function. From the computational point of view, the present approach is more advantageous, as it is compatible with most standard direct CI algorithms requiring expansions defined by orbital occupation numbers within subspaces. Furthermore, we can take advantage of the natural extensions of the CAS approach, such as GAS, in order to treat FCI problems of large dimensionality. As we will show in the following, with the SplitGAS method, we have been able to achieve chemical accuracy for strong-correlation problems bypassing any PT2 correction of multiconfigurational reference functions, a remarkable result.

The paper is organized as follows: In section II we describe the formulation of the method. In section III we discuss the computational details and results for the HF, N_2, and Cr_2 molecules, and, finally, in section IV, we offer the concluding remarks.

II. FORMULATION

The theory of the SplitGAS method is described in the original paper.[30] We summarize here the most important concepts and the formulation of the orbital-based partitioning.

The definition of a wave function expansion in terms of splitting of the orbitals into subspaces encompasses many forms of CI-expansions. A simple choice of orbital sets is obtained by first performing an orbital optimization for a reference state consisting either of a Hartree−Fock or a CAS state and then dividing the resulting orbitals in five sets: an inactive set, a secondary set, and three other sets of orbitals:

(O) A space containing doubly occupied orbitals,

(A) A space containing some doubly occupied and some virtual orbitals. It may coincide with the active space of the reference state, if relevant.

(V) A space containing only virtual orbitals.

The orbital splitting is represented in Scheme 1. The (A) space is a small active space, while the full (O)+(A)+(V) space

Scheme 1. Orbital Splitting Employed in the Definition of a SplitGAS Wave Function

Space 5		Secondary		Secondary
Space 4		Secondary (V)		Active
Space 3	:	Active (A)	→	Active
Space 2		Inactive (O)		Active
Space 1		Inactive		Inactive

can be considered as a larger active space. All configurations generated by excitations within the (A) space, by keeping the orbitals in (O) doubly occupied and the orbitals in (V) empty, form the principal space (P) of the CI-expansion, whereas all configurations generated by single and double excitations out of the (O) space and (A) space into the (V) space belong to the extended space (Q) of the SplitGAS wave function. The extended space (Q) hence plays an analogous role as a perturbation to the primary space (P) and recovers the remaining electron correlation, that can be both static and/or dynamic.

The above orbital based partitioning scheme may be further refined using other variants of the active space concept. For instance, the user could use a RAS wave function as a reference state, thereby dividing the above (A) space into three spaces. The RAS wave function may then be chosen as the (P) space, whereas the (Q) space is obtained by allowing varying occupations in the five orbital spaces reported in Scheme 1.

By appropriate choices of the number of active spaces and occupation number constraints, the user can perform any partition of the CI-expansion, according to the chemistry of the system under investigation. Only the most important configurations will effectively contribute to the CI expansion in the principal and extended space. In the GAS approach, one can in principle choose an arbitrary number of orbital spaces, and, as a consequence, the size of the problem does not exhibit the exponential scaling as a function of the number of electrons

dx.doi.org/10.1021/ct400046n | J. Chem. Theory Comput. XXXX, XXX, XXX−XXX

and orbitals included in the various spaces, which makes the CAS approach unfeasible for large active spaces. Through the GAS choice, the principal space contains only the most important configurations, while the other non-negligible configurations are included in the extended space, and the "dead-woods" generated from the CI-expansion can be, if not eliminated, at least significantly reduced. This approach bypasses thereby the scaling problems in terms of number of operations and memory requirements of CI expansion in CAS-type of calculations.

Both SplitGAS-CI and SplitGAS-SCF variants have been developed. The former consists of the optimization of the CI parameters only, while the latter combines the optimization of both the CI coefficients and the orbitals. In this paper, we focus on the SplitGAS-CI variant. We tested the SplitGAS method on three systems, which pose increasing challenges as far as electron correlation is concerned, namely the HF, N_2, and Cr_2 molecules.

With the SplitGAS method the eigenvalue E and eigenvector of the dressed matrix U with elements

$$U_{mn} = H_{mn} - \sum_{\gamma} \frac{H_{m\gamma}H_{\gamma n}}{H_{\gamma\gamma} - E} \tag{1}$$

are determined. In eq 1 m and n refer to configuration state functions (CSFs) of the principal (P) space, whereas γ is a CSF of the extended (Q) space. The matrix-elements H_{pq} are thus matrix elements between two configuration state functions (CSFs) of the Hamiltonian operator

$$\hat{H} = \sum_{kl} h_{kl}\hat{E}_{kl} + \frac{1}{2}\sum_{ij,kl} (ijlkl)(\hat{E}_{ij}\hat{E}_{kl} - \delta_{jk}\hat{E}_{il}) \tag{2}$$

where h_{kl} and $(ijlkl)$ are integrals over molecular orbitals of the one- and two-body Hamiltonian, respectively, and $\hat{E}_{kl}$ is a spin-free one-body excitation operator. Equation 1 represents Löwdin's original formulation[31] approximated to the second-order of the geometrical expansion (diagonal approximation).

Since SplitGAS belongs to the category of approximated CI methods, it is not strictly size-extensive. However, in a calculation the orbital spaces and occupations can be defined and tailored in such a way that the CI-energies of the subsystems and supersystem match.

Although the dimension of U is much smaller than the dimension of the full matrix H, it is necessary to invoke direct CI methods to obtain the eigensolutions of U. In the direct CI formulation of the SplitGAS method a sigma vector of size (P) is obtained from the dressed Hamiltonian matrix U as

$$\sigma_m = \sum_{n}^{P} U_{mn}C_n = \sum_{n}^{P}\left(H_{mn} - \sum_{\gamma}^{Q} \frac{H_{m\gamma}H_{\gamma n}}{H_{\gamma\gamma} - E}\right)C_n \tag{3}$$

The direct CI vector may alternatively be written in matrix form as

$$\sigma^P = [H^{PP} - H^{PQ}(H^{QQ}_{diag} - E)^{-1}H^{QP}]C^P \tag{4}$$

The direct CI vector of eq 4 may in principle be calculated by storing only vectors of P-size. We have, however, initially adopted an approach where two vectors over the (Q) space are also stored. We have thus implemented in a local version of the LUCIA[38] code the following algorithm.

- compute $H^{PP}C^P$ and save on scratch file 1 (size of P)
- compute $H^{QP}C^P$ and save on scratch file 2 (size of Q)
- compute H^{QQ}_{diag} and save on scratch file 3 (size of Q)
- compute $(H^{QQ}_{diag}-E)^{-1}H^{QP}C^P$ and save on scratch file 2
- compute $H^{PQ}(H^{QQ}_{diag}-E)^{-1}H^{QP}C^P$ and save on scratch file 3
- Combine vectors on scratch files 1 and 3 to obtain σ^P

For computational simplicity and efficiency the direct CI calculations of the sigma-vectors are carried out using Slater determinants (SDs), whereas to reduce disk-space the vectors are stored in the Configuration State Function (CSF) basis. For the evaluation of the sigma vectors as well as the CSF-SD transformations, the standard routines of LUCIA are used without modifications. It is worth mentioning that at no time is it necessary to store in memory a complete vector in the (P) or (Q) space. Rather the program uses the standard facility of LUCIA to separate the C- and sigma-vectors into batches and having only one batch of C and sigma in memory at any given time. As CSFs here are employed, a batch contains at least the CSFs or SDs of a given occupation class, where an occupation class contains all CSFs or SDs with a given number of electrons in each GA space. Thus by increasing the number of GA spaces, a given expansion may be divided into a larger number of smaller batches, and the memory requirement is reduced. This reduction is accompanied by an increase in the CPU wall-time of usually less than 30%. This facility was important in the calculations discussed below with up to about 2 billion determinants in the (Q) space. It should be noted that the memory requirements could be further reduced if only SDs were used, as this would only require batches holding the alpha- and beta-strings with given occupations in each GA space.

The computational complexity in a SplitGAS calculation may for simple expansions easily be compared with the preceding reference calculation. Assume that the reference expansion is a FCI calculation with $M_S = 0$ and n_P electrons in N_P orbitals, whereas the active orbital space of the (Q) space is obtained by adding a set of N_Q unoccupied orbitals. A direct CI iteration in the (P) space, i.e. the evaluation of H^{PP} times a vector, requires a number of floating points operations which through leading order is proportional to ${n_P}^2(N_P-n_P/2)^2\ {N^P}_{det}$, where ${N^P}_{det}$ is the number of determinants in the P-expansion. Each iteration in the SplitGAS approach requires the evaluation of H^{PQ} times a vector. The block H^{PQ} includes all single and double excitation out of N_P orbitals in the P-expansion into N_Q orbitals giving an operation count that is proportional to ${n_P}^2\ {N_Q}^2\ {N^P}_{det.}$ Thus, the evaluation of H^{PQ} times a vector requires about ${N_Q}^2/(N-n_P/2)^2$ times the operations of the evaluation of H^{PP} times a vector. Consider as an example the Cr_2 calculations discussed in section III, with $n_P = N_P = 12$, and $N_Q = 40$ (Cr_2 SplitGAS-2(12,12)//(12,52)) where the evaluation of the H^{PQ} terms thus is predicted to be 44 times more time-consuming than the underlying FCI iteration. For a larger number of orbitals correlated in the (Q) space and when additional numbers of electrons are correlated in the extended space, the evaluation of the H^{PQ} term may be at least 2 orders of magnitude more demanding than the preceding FCI iteration.

The second part of the computation is the evaluation of the diagonal of H^{QQ}. To determine the complexity of this evaluation, it is first noted that the number of determinants in the (Q) space, ${N^Q}_{det}$, through leading order equals $1/2\ {N_Q}^2{n_P}^2/(N_P-n_P/2)^2{N^P}_{det}$. The determination of the diagonal of the Hamiltonian matrix in the determinant basis requires a double sum over occupied orbitals for each determinant, giving a total operation count proportional to ${N_Q}^2{n_P}^4/(N_P-n_P/2)^2{N^P}_{det}$, corresponding to a factor ${n_P}^2/(N_P-n_P/2)^4$ times the operation count for constructing a direct CI vector for H^{PQ}. For

dx.doi.org/10.1021/ct400046n | J. Chem. Theory Comput. XXXX, XXX, XXX−XXX

typical expansions n_P is about N_P, so the diagonal in the determinant basis is less costly to construct than the evaluation of terms of H^{PQ}. The evaluation of the diagonal in the CSF basis is more requiring than in the SD basis with a factor that increases with an increasing number of open orbitals in the various configurations, so in total, the evaluation of the diagonal terms may be as or more requiring than the evaluation of the terms from H^{PQ}. The transformation between the SD and CSF basis was neglected in the above, but in particular the transformation for vectors in the (Q) space may be a sizable part of the iteration time, due to the large dimensions in this space.

A direct CI iteration with the dressed U-matrix of eq 1 is thus typically at least 2 orders of magnitude more demanding than direct CI iteration in the (P) space. On the other hand, a direct CI iteration with the full Hamiltonian in the P+Q space has an operation count that scales as $N_Q{}^2N^Q{}_{det}$ or $N_Q{}^4n_P{}^2/(N_P-n_P/2)^2N^P{}_{det}$ and is typically 1 or 2 orders of magnitude larger than that of that of the evaluation of terms from U. A direct comparison of the complexity of the present approach and the standard CASPT2 calculation is not straightforward, as the latter approach in general uses internal contractions. If the present approach were to be reformulated into an internal contraction scheme and the full orbital space were used, the complexity of the two approaches would be similar.

In the above, the complexity was discussed in terms of operation counts. However, with the advance of multicore CPUs and multi-CPU computers, the importance of operation counts is reduced, and it is important to also include considerations of concurrency and data-communication. In the SplitGAS approach, only vectors with dimension $N^P{}_{det}$ need to be stored and communicated to the various cores, so the storage and communication requirements depend solely on the size of the (P) space. Furthermore, using batching of the (P) and (Q) space, the computational task of evaluating a sigma-vector may be divided into a large number of independent smaller computational tasks. The SplitGAS method with its small requirements on storage and communication and high degree of concurrency is therefore well suited to exploit modern parallel computer facilities.

III. COMPUTATIONAL DETAILS AND RESULTS

Potential energy curves for the ground state of the HF, N_2, and Cr_2 molecules were generated with several SplitGAS choices and compared with Restricted HF, MP2, CASCI, CASSCF, CASPT2, GASCI, GASSCF, and experimental counterparts. Spectroscopic parameters were computed by solving the numerical Schrödinger equation as implemented in the module VIBROT available in MOLCAS-7.7[18] and compared to available experimental values. Dissociation energies were computed as energy differences between the diatomic at equilibrium and the diatomic with the two atoms at large separation (R > 100 Å).

A preliminary calculation is needed to obtain starting orbitals. The necessary one- and two-electron integrals, transformed from the atomic orbital basis to the molecular orbital basis, are generated by the MOTRA module in MOLCAS-7.7[18] and used by the SplitGAS algorithm implemented in the LUCIA code.[38]

The following notation is used for SplitGAS calculations: SplitGAS-$m(N_P,n_P)//(N_T,n_T)$ where m is the number of GA spaces, N_P and n_P are the number of active electrons and active orbitals in (P) space, and N_T and n_T are the number of active electrons and orbitals in (P+Q).

A. The HF Molecule. For the HF molecule, potential energy curves were computed using the cc-pVDZ basis set (H:2s1p, F:3s2p1d, 19 basis functions in total)[39] and by imposing C_{2v} point group symmetry constraints. Selected calculations were also performed with the cc-pVTZ and cc-pVQZ basis sets. Two SplitGAS partitions were employed. In the first scheme, SplitGAS-2(8,4)//(8,18), the principal (P) space includes the Restricted Hartree−Fock configuration $(1s^22s^22p_x{}^22p_y{}^2)_F\ \sigma^2{}_{HF}$, with single and double excitations out of the $2s_{(F)}$ and $2p_{(F)}$ orbitals into all 14 virtual orbitals representing the extended (Q) space (1 Slater determinant in (P) and 1174 Slater determinants in (Q) space). For this scheme Restricted HF orbitals were used as starting orbitals. In the second test case, SplitGAS-3(2,2)//(8,18), the principal (P) space is generated by a CAS(2,2) where the two active orbitals are the bonding and antibonding sigma-type orbitals, and the extended space is generated by single and double excitations out of the $2s_{(F)}$, $2p_{x(F)}$, and $2p_{y(F)}$ orbitals and/or into the remaining 13 virtual orbitals (4 Slater determinants in (P) space and 3780 Slater determinants in (Q) space). The $1s_{(F)}$ orbital was kept inactive in both SplitGAS schemes.

The SplitGAS calculations were compared to (i) Restricted Hartree−Fock, RHF, (ii) MP2, (iii) CASSCF(2,2), where the two active orbitals are the σ and σ^* orbitals, (iv) CASPT2(2,2), (v) CASSCF(8,18) calculations (note that this is almost a full CI except that the $1s_{(F)}$ orbital is inactive), (vi) GASCI-2(8,4)//(8,18)SD calculations, in which the $1s_{(F)}$ orbital was kept inactive, starting from RHF orbitals, and only single and double excitations were considered, and (vii) available experimental data.[40,41] One should notice that, instead of using a diagonal approximation for the (QQ) block of the CI Hamiltonian matrix, as done in SplitGAS, in GASCI there is no approximation of the CI Hamiltonian matrix. In the GASCI-2(8,4)//(8,18) calculations all the states are coupled among each other, while in SplitGAS-2(8,4)//(8,18) only the restricted-HF configuration is explicitly coupled (through the PQ and QP blocks) to the single and double excited configurations. This is the effect of the diagonal approximation in the (QQ) block.

Potential energy curves are presented in Figure 1, and spectroscopic parameters for selected curves are presented in Table 1. Not surprisingly, RHF and MP2 predict the wrong ionic dissociation. Single and double excitations from the RHF wave function, GASCI-2(8,4)//(8,18)SD, partially improve the description of the system at dissociation. CASSCF(2,2) significantly underestimates the dissociation energy. CASPT2-(2,2) improves the description. It is interesting to notice the slow convergence of CASPT2 with the basis set. SplitGAS-2(8,4)//(8,18), in which single and double excitations to the virtual orbitals are included perturbatively, and only the Hartree−Fock configuration constitutes the principal (P) space, overestimates the dissociation energy (D_e) by 0.47 eV with respect to the corresponding GASCI-2(8,4)//(8,18)SD result. SplitGAS-3(2,2)//(8,18) predicts an equilibrium bond distance and dissociation energy in good agreement with experiment. Moreover, with a double-ζ quality basis sets, it produces values comparable with those obtained at the CASPT2 level with a quadruple-ζ basis set. However, it overestimates the dissociation energy and underestimates the equilibrium bond distance when compared to the CAS(8,18) method.

B. The N_2 Molecule. For the N_2 molecule, the cc-PVQZ basis set (N:5s4p3d2f1g) and the D_{2h} point group were

dx.doi.org/10.1021/ct400046n | J. Chem. Theory Comput. XXXX, XXX, XXX−XXX

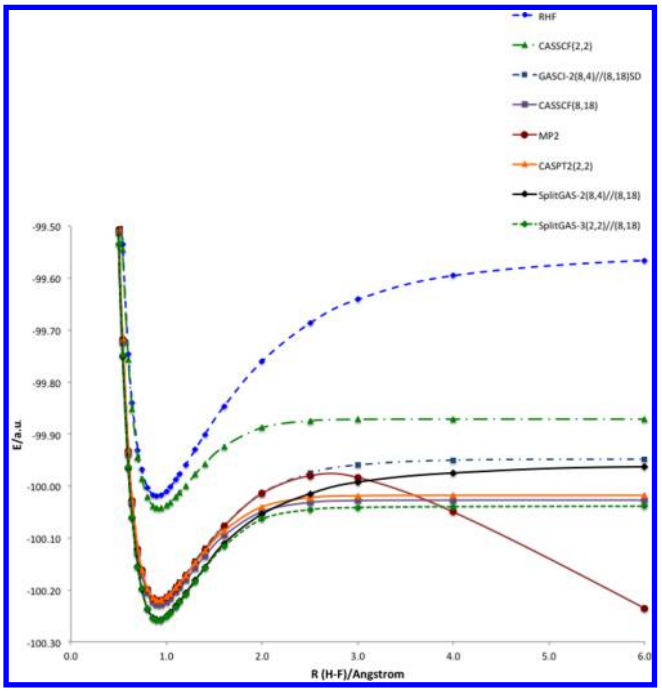

Figure 1. HF potential energy curves.

employed. At equilibrium, N_2 has a triply bonded singlet ground state, which dissociated into two N ($1s^2 2s^2 2p^3$) atoms. A minimal active space includes six electrons distributed in six orbitals, CAS(6,6).

For this system we performed: (i) restricted-HF calculations, (ii) MP2, (iii) GASCI-2(10,5)//(10,12)SDT, in which two GA spaces were chosen, one containing the five doubly occupied valence orbitals and the other one containing seven low-lying correlating virtual orbitals. Up to triple interspace excitations were used to generate the CI space, (iv) analogous GASCI but including up to sextuple excitations, GASCI-2(10,5)//(10,12)-SDTQ56, (v) CASSCF(6,6) calculations, (vi) CASPT2(6,6), (vii) CASSCF(10,14), including two additional doubly occupied orbitals, mainly with 2s character on each N atom, and six more virtual orbitals, (viii) CASPT2(10,14), and (ix) four different SplitGAS schemes (vide infra).

We also performed the corresponding GASSCF calculation for scheme (iii), GASSCF-2(10,5)//(10,12)SDT, to check if orbital optimization recovers part of the correlation missed by a truncated level of excitation.

In one of the SplitGAS schemes, only the HF configuration was included in the principal space (P), while the configurations arising from single and double excitations from the five valence bonding orbitals to the seven low-lying virtual orbitals were included in the extended (Q) space (1 Slater determinant in (P) space and 245 in (Q) space). We will refer to this calculation as SplitGAS-2(10,5)//(10,12). In the other three cases a CAS(6,6) expansion was chosen for the principal space (56 Slater determinants), while the extended orbital space was different. In one case, SplitGAS-3(6,6)//(10,12), 13894 Slater determinants of the (Q) space couple with the principal space. In the second case, SplitGAS-3(6,6)//(10,24) 192898 Slater determinants of the extended space couple with the principal space. In the last case, SplitGAS-3(6,6)//(14,26), the extended space included also single and double excitations from the 1s orbitals, This choice leads to 659544 Slater determinants coupling with the principal space. Optimized CAS(6,6) natural orbitals were used as input orbitals for the SplitGAS calculations. We also performed GASCI-type of calculations to directly compare them with the SplitGAS calculations. The optimized CAS(6,6) natural orbitals were used, and starting from them an enlarged CI space was generated, namely a GAS-3(6,6)//(10,12)SD, a GAS-3(6,6)//(10,24)SD, and a GAS-3(6,6)//(14,26)SD. Instead of using the diagonal approximation in the (QQ) block of the CI Hamiltonian matrix, in the GASCI calculations no approximation of the CI Hamiltonian matrix was employed. The experimental data are taken from ref 42.

Selected potential energy curves are presented in Figure 2, and selected spectroscopic parameters are reported in Table 2.

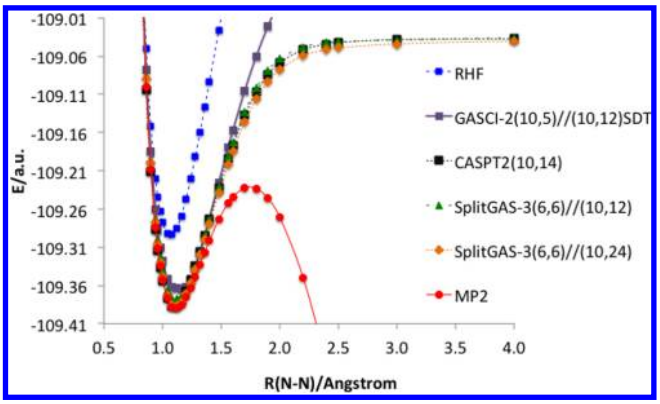

Figure 2. N_2 potential energy curves.

Both RHF and MP2 predict the wrong dissociation energy. GASCI (GASCI-2(10,5)//(10,12)SDT) up to triple excitations

Table 1. HF Spectroscopic Constants[a]

method	R_{eq} (Å)	D_e (eV)	D_o (eV)	ω_e (cm^{-1})	$\omega_e x_e$ (cm^{-1})
RHF	0.902	12.87	12.60	4454.5	97.7
CASSCF(2,2)	0.921	4.68	4.43	4071.4	110.2
CASPT2(2,2)	0.920	5.49	5.24	4159.5	102.1
CASPT2(2,2) cc-pVTZ	0.917	5.94	5.68	4201.1	96.9
CASPT2(2,2) cc-pVQZ	0.915	6.06	5.81	4203.6	99.5
GASCI-2(8,4)//(8,18)SD	0.917	7.39	7.13	4219.7	94.0
SplitGAS-2(8,4)//(8,18)	0.911	7.86	7.58	4558.9	261.8
SplitGAS-3(2,2)//(8,18)	0.915	6.01	5.74	4362.3	148.4
CASSCF(8,18)	0.920	5.49	5.23	4144.2	102.1
exp.[40,41]	0.917	6.12		4138.7	90.1

[a]Unless otherwise specified, the basis set used is cc-pVDZ.

dx.doi.org/10.1021/ct400046n | J. Chem. Theory Comput. XXXX, XXX, XXX−XXX

Table 2. N_2 Spectroscopic Constants Obtained Using the cc-PVQZ Basis Set

method	R_{eq} (Å)	D_e (eV)	D_o (eV)	ω_e (cm^{-1})	$\omega_e x_e$ (cm^{-1})
RHF	1.066	33.13	32.97	2730.4	111.9
GASCI-2(10,5)//(10,12)SDT	1.162	18.00	17.02	1301.3	749.3
GASSCF-2(10,5)//(10,12)SDT	1.096	19.83	19.68	2412.6	106.7
CASSCF(6,6)	1.102	8.80	8.75	2351.7	142.5
CASSCF(10,14)	1.097	9.85	9.70	2387.8	142.6
CASPT2(10,14)	1.101	9.55	9.40	2340.8	153.6
SplitGAS-3(6,6)//(10,12)	1.106	9.28	9.14	2364.1	462.2
SplitGAS-3(6,6)//(10,24)	1.110	9.53	9.39	2296.7	111.6
SplitGAS-3(6,6)//(14,26)	1.110	9.55	9.41	2298.4	111.8
exp[42]	1.098	9.76		2358.6	

does not correctly dissociate N2, because not all the relevant excitations are included in the CI expansion, which is still dominated by configurations with ionic character. Orbital optimization coupled to this CI expansion (GASSCF-2(10,5)//(10,12)SDT) does not solve the problem.

The CASSCF(6,6) calculation predicts a dissociation energy of 8.80 eV, ca. 1 eV lower than the experimental value. By including two doubly occupied orbitals, mainly N 2s, and six virtual orbitals for correlation, CASSCF(10,14), the results improve significantly. Inclusion also of a perturbative correction to the second-order, CASPT2(10,14) gives results in good agreement with experiment.

For the SplitGAS-2(10,5)//(10,12), (these results are not reported) in which only the HF configuration is included in the principal partition of the CI expansion with all single and double excitations to the seven low-lying correlating virtual orbitals forming the extended space, we experienced convergence problems at bond distances greater than 3.0 Å. This arises from the fact that at dissociation some important configurations were left into the extended space. This observation stresses that all the important configurations along the reaction path must be included in the principal space to guarantee the trustworthiness of the method and to avoid convergence problems. All SplitGAS results for this system give equilibrium bond lengths, vibrational frequencies, and dissociation energies of CASPT2 quality.

A direct comparison of the GASCI curves and the analogous SplitGAS curves is shown in Figure 3, and the spectroscopic parameters are summarized in Table 3.

While the SplitGAS curves overlap with the corresponding GASCI curves near the equilibrium region, they differ at

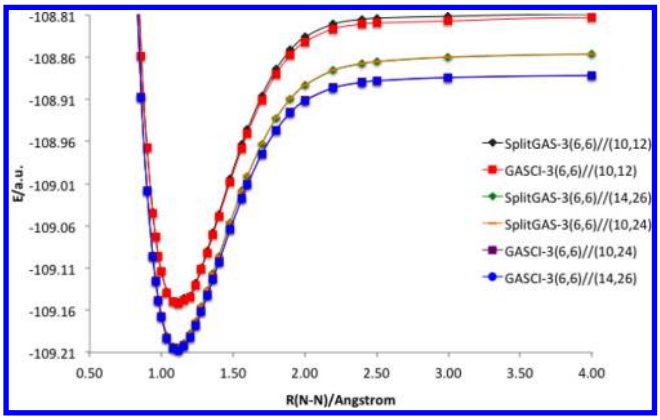

Figure 3. N_2 potential energy curves: comparison of the SplitGAS and GASCI methods.

Table 3. N_2 Spectroscopic Constants: Comparison of SplitGAS and GASCI (Basis Set: cc-PVQZ)

method	R_{eq} (Å)	D_e (eV)	D_o (eV)	ω_e (cm^{-1})
GASCI-3(6,6)//(10,12)SD	1.108	9.12	8.99	2288.0
SplitGAS-3(6,6)//(10,12)	1.106	9.28	9.14	2364.1
GASCI-3(6,6)//(10,24)SD	1.111	8.88	8.74	2276.0
SplitGAS-3(6,6)//(10,24)	1.110	9.53	9.39	2296.7
GASCI-3(6,6)//(14,26)SD	1.111	8.89	8.75	2277.7
SplitGAS-3(6,6)//(14,26)	1.110	9.55	9.41	2298.4

dissociation. The reason for this difference is that at dissociation part of the correlation energy is neglected with SplitGAS, because of the diagonal approximation for the (QQ) block. As a result, SplitGAS slightly overestimates the dissociation with respect to GASCI. In this case we can therefore conclude that SplitGAS is closer to the experimental value than the GASCI counterpart, due to cancellation of error.

The SplitGAS-3(6,6)//(10,24) and SplitGAS-3(6,6)//(14,26) curves almost overlap. The same behavior is encountered for the GASCI curves. This indicates that the coupling between core electrons and valence orbitals for this system is small.

Instead of natural orbitals, canonical orbitals could also be used as starting orbitals for the SplitGAS calculations. For the systems under investigation, canonical and natural orbitals are almost identical. In general, however, these two sets of orbitals may significantly differ, and the choice of one set or the other as starting orbitals in a SplitGAS calculation might bring to a different result.

As a final note to this section, we would like to note that the discrepancy between SplitGAS and GASCI is much larger for HF (Section A) than for N_2 (Section B). The reason for this difference is that in the N_2 calculations the reference wave function is a CAS(6,6). The additional configurations included perturbatively in SplitGAS and explicitly in GASCI account for the missing dynamic correlation. For the HF system, on the other hand, we used restricted-HF as a reference wave function, which is not as accurate as the reference wave function used for N_2.

C. The Cr_2 Molecule. The Cr_2 molecule[43,44] is a challenging system for modern electronic structure theory methods because it is highly multiconfigurational and both static and dynamic correlations play an important role. For this molecule, the ground state singlet potential energy curve was computed using the ANO-RCC basis set[45] with a VTZP (TZP, 6s5p3d2f1g) and D_{2h} point group. The Douglas-Kroll-Hess Hamiltonian[46,47] was employed to account for scalar relativity. Since the Cr atom has a high-spin $^7S_3$ ground state and a $(3d)^5(4s)^1$ valence

dx.doi.org/10.1021/ct400046n | J. Chem. Theory Comput. XXXX, XXX, XXX−XXX

configuration, a complete spin pairing of two Cr atoms can formally produce a hextuple bonded system.[48−51] A minimal active space includes 12 electrons distributed in 12 orbitals, the 3d and 4s on each Cr atom, CAS(12,12). Calculations at the CASSCF(12,12) and CASPT2(12,12) levels are presented. For the CASPT2 an imaginary shift of 0.2 au was chosen together with an IPEA value of 0.45 au, which are considered the best parameters for the Cr_2 system.[52] Orbitals up to the 3s were kept frozen in the CASPT2 correction. CASPT2 calculations were also performed with a larger ANO-RCC-type basis set, namely the 21s15p10d6f4g2h basis contracted to a 10s10p8d6f4g2h basis (7ZP because it is of septuple-zeta quality) and both CASPT2 and SplitGAS calculations with a smaller basis set, namely ANO-RCC-VDZP (DZP, 5s4p2d1f).

Four SplitGAS schemes were used, in which optimized CASSCF(12,12) natural orbitals were employed, and the principal (P) space included the whole CAS(12,12) CI expansion. The four SplitGAS calculations differ in the size and partitioning of the active space. In the smallest SplitGAS case, two GA spaces were included, one including the twelve valence orbitals, the other including 18 virtual orbitals, which are used for the extended (Q) space, SplitGAS-2(12,12)//(12,30). These 18 orbitals are the bonding and antibonding combinations of the three 4p components, the 5s, $5p_z$, 4dσ, the two 4dδ and the 4fσ atomic orbitals, and were selected as the virtual canonical orbitals of correct symmetry with the lowest energy. The rationale behind this choice was to include orbitals that are primarily in the bonding region. The δ-orbitals were all included as some of them, within the D_{2h} point group, shared the same irreducible representation with the σ-orbitals. Single and double excitations of the 12 active electrons into the 18 virtual orbitals were allowed. In the second test, the extended orbital space was further enlarged: SplitGAS-2(12,12)//(12,52). Among the virtual orbitals we added bonding and antibonding combinations of the $5p_x$, $5p_y$, 6s, 4dπ, 5dσ, 5dδ, 4fπ, and 4fδ atomic orbitals. The added orbitals were again chosen as the virtual canonical orbitals of correct symmetry with lowest energy. The two first SplitGAS expansions consider therefore only correlation of the valence orbitals. In the third expansion, three GA orbital spaces were employed: one space containing the two doubly occupied $3p_z$ orbitals, the second space containing the twelve valence orbitals, and the third space containing twenty correlating virtual orbitals. Single and double excitations were allowed from the $3p_z$ orbitals and/or into the twenty extended virtual orbitals. We refer to this calculation as SplitGAS-3(12,12)//(16,34). This expansion allows therefore for a partial description of core−core, core−valence, and valence correlation effects.

In the largest SplitGAS expansion, all electrons in the 3p-, 3d-, and 4s- derived orbitals were correlated. This was accomplished by selecting a first GA space containing the six molecular orbitals originating from 3p, a second GA space containing the 12 molecular orbitals originating from 3d, 4s, and a third orbital space containing 30 correlating orbitals. The orbitals in the first and third space were again canonical orbitals and were chosen as the inactive with highest orbital energy and the virtual orbitals with lowest energy, respectively. In order to reduce memory requirements, the last orbital space was actually divided into four orbital spaces, so a total of six active orbital spaces were actually used, and we refer to this calculation as SplitGAS-6(12,12)//(24,48). The six orbital spaces are described in Table 4.

Table 4. Number of Orbitals in Each Irrep of D_{2h} in the SplitGAS-6/(12,12)//(24,48) Calculation

irrep	a_g	b_{3u}	b_{2u}	b_{1g}	b_{1u}	b_{2g}	b_{3g}	a_u
GAS1	1	1	1	0	1	1	1	0
GAS2	3	1	1	1	3	1	1	1
GAS3	7	0	0	0	7	0	0	0
GAS4	0	3	0	0	0	3	0	0
GAS5	0	0	3	0	0	0	3	0
GAS6	0	0	0	2	0	0	0	2

The (Q) space was defined as the CSFs with at most one hole in the first GA space and at most two electrons in last four GA spaces. This expansion includes therefore core−valence as well as valence correlation effects.

It is well-known that CASSCF(12,12) calculations do not reproduce the qualitative features of the exact potential energy curve, see also Figure 4. The reason for this failure is the lack of

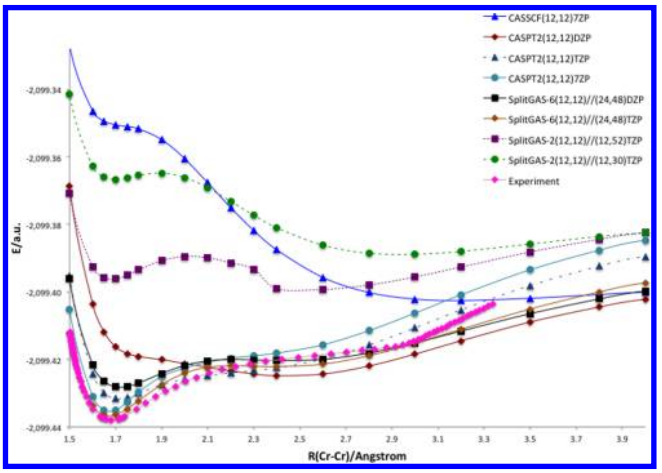

Figure 4. Cr_2 potential energy curves. The curves are arbitrarily shifted for better comparison (for absolute values see the Supporting Information).

dynamic correlation in these calculations. Dynamic correlation for this molecule has been traditionally recovered by the CASPT2 approach. Several Cr_2 CASPT2 potential energy curves have been proposed over the years, corresponding to different parametrizations of the method. The original CASPT2 curve[53] was affected by a severe intruder-state problem, which 'deteriorated' the result. Using the level-shift technique in the LS-CASPT2 method,[10] the intruder-state problem was partially solved, but a first parameter was introduced. An imaginary level-shift was also employed as an alternative solution to the intruder states problem.[11] The most recent parametrization was introduced as a shifted zeroth-order Hamiltonian (IPEA shift).[12] This approximation corrects for the systematic error of the original formulation, where the correlation energy was overestimated. The shape of the potential energy curve of the Cr_2 is affected by the choice of this new parameter,[52] which leads to different spectroscopic parameters. SplitGAS avoids any empirical or semiempirical parametrization. The only choice that one has to make is the active space in the principal (P) and extended (Q) space.

Selected potential energy curves for Cr_2 are plotted in Figure 4. A closer view of the CASPT2, SplitGAS-6(12,12)//(24,48), and experimental curves is presented in Figure 5. The spectroscopic constants are reported in Table 5. The calculated

dx.doi.org/10.1021/ct400046n | J. Chem. Theory Comput. XXXX, XXX, XXX−XXX

and experimental vibrational frequencies are reported in Table 6.

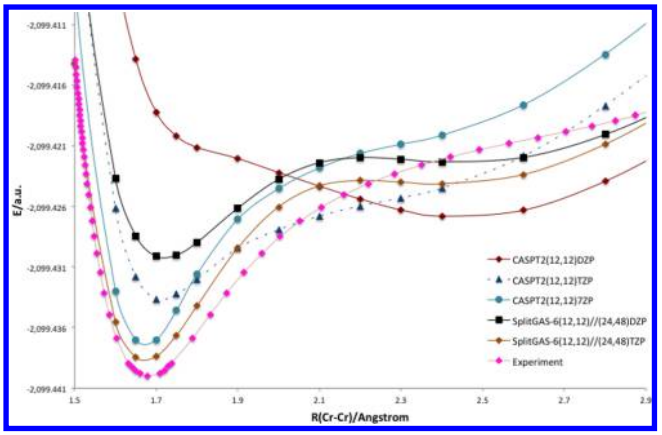

Figure 5. Enlarged region for selected Cr_2 curves. The curves are arbitrarily shifted for better comparison (for absolute values see the Supporting Information).

Table 5. Cr_2 Spectroscopic Constants for Selected Methods

method	R_{eq} (Å)	D_o (eV)	ω_e (cm^{-1})
CASPT2 (12,1,2)/DZP	no min	-	-
CASPT2 (12,1,2)/TZP	1.713	1.39	309.1
CASPT2 (12,1,2)/7ZP	1.673	1.59	505.8
SplitGAS-6(12,12)//(24,48)/DZP	1.720	1.17	324.9
SplitGAS-6(12,12)//(24,48)/TZP	1.671	1.56	484.8
exp[44]	1.679	1.44 ± 0.05	480.6 ± 0.5

Table 6. Cr_2 Lowest Vibrational Levels

v	CASPT2/TZP	CASPT2/7ZP	SplitGAS/TZP	exp[44]
1	401	563	476	452
2	334	519	450	423
3	266	461	416	405
4	208	394	382	365
5	175	334	350	340
6	146	280	316	315
7	126	239	278	280
8	119	207	228	250
9	119	176	86	210

In Figure 4 we report the curve for the CASSCF(12,12) calculations only with the largest basis set, 7ZP. This potential energy curve as well as the CASSCF(12,12) potential energy curves for the other basis sets (not given in Figure 4) predicts an unbounded Cr_2 ground state. At the CASPT2(12,12)/DZP level the curve does not have a minimum. At the CASPT2-(12,12)/TZP level, the system is predicted to be bonded, with an equilibrium bond length of 1.71 Å, a dissociation energy of 1.39 eV, and a vibrational constant ω_e of 309 cm^{-1}. Overall the curve is flatter than the experimental one. By increasing the basis set to 7ZP, the CASPT2(12,12) results improve significantly. The equilibrium bond distance agrees with the experimental value. The dissociation energy and ω_e values are slightly overestimated; the minimum is deeper and narrower compared to the experimental one (Figure 5).

Let us now consider the SplitGAS calculations. Inspection of Figure 4 shows that all the SplitGAS curves present a local minimum at short distance, corresponding to the 3d-3d interaction. However, only calculations including core-correlation from all six 3p-derived orbitals, i.e. the calculations with the (P)+(Q) active space of twenty-four electrons in forty-eight orbitals, (24,48), reproduce the experimental curve, while the other expansions (12,30), (12,52), and (16,34) without or with only partial core−valence correlation energy, do not predict an overall correct shape of the curve.

Figure 5 shows that the SplitGAS-6(12,12)//(24,48)/TZP curve nicely overlaps with the experimental curve near the equilibrium region, from 1.4 Å to 2.4 Å. The SplitGAS-6(12,12)//(24,48) shoulder is more enhanced than the experimental one. A shallow second minimum appears at 2.404 Å on the SplitGAS curve. The difference between the experimental and SplitGAS-6(12,12)//(24,48) curves in the region between 2.4 Å and 3.0 Å is not of particular concern; as pointed out already by the authors of the experimental study,[45] insufficient experimental vibrational data are available to allow an accurate experimental fitting in that region of the curve. The presence of the shallow minimum obtained with the SplitGAS-6(12,12)//(24,48) method is therefore not to be excluded.

The spectroscopic parameters obtained with the SplitGAS-6(12,12)//(24,48) method match the experimental values (Table 5). The SplitGAS-6(12,12)//(24,48) vibrational frequencies (Table 6) are in better agreement with the experimental values than the CASPT2 ones obtained with the largest basis set. In Table 6 we reported only the first nine vibrational levels because these are those accurately determined experimentally and represent a good reference for the theoretical counterparts. Already for v = 9 the deviation of the SplitGAS-6(12,12)//(24,48) frequency from the value reported in ref 44 is large, probably because this vibrational level is already in the nonaccurate experimental region.

We have compared calculations with DZP and TZP basis sets, in order to investigate basis set effects. The CASPT2/DZP curve does not have a minimum at short distance (1.7 Å). The CASPT2/TZP curve, on the other hand, has a correct shape. The SplitGAS/DZP curve has a similar shape as the CASPT2/TZP near the first minimum, while it is more similar to the CASPT2/DZP curve at large distance. Overall, with our choices of orbital spaces, already at the DZP level the SplitGAS curve is qualitatively correct, and, at the TZP level, it perfectly overlaps with the experimental curve, in the region that has been accurately measured.

IV. CONCLUDING REMARKS

We have presented a new method, SplitGAS, that generates accurate multiconfigurational wave functions at an affordable cost. The GAS CI-expansion is split into two parts, a principal part containing the most relevant configurations and an extended part containing less relevant (but not negligible) configurations. The partition is based on an orbital criterion. The SplitGAS approach has several advantages over existing electronic structure methods for strong correlation:

- It gives equilibrium bond lengths, vibrational frequencies, and dissociation energies of CASPT2 quality at computational costs that in each iteration are similar to those of (uncontracted) CASPT2 calculations but with memory requirements that are similar to those of CASSCF.
- The construction of the wave function is based on the active space choice, which requires exclusively chemical knowledge of the given system. This implies that accurate results can be obtained only upon careful selection of the

configurations included. Therefore, the method is not black-box.

- Unlike PT2-type methods, it is free from any parametrization of the Hamiltonian.
- With small to middle size basis sets it gives results with chemical accuracy. From this point of view the method might benefit from cancellation of errors with the small basis sets.
- The SplitGAS method is not per se size-extensive. However, the orbital spaces and occupations constraints of a supersystem consisting of noninteracting subsystems may be specified in such a way that the energy of the supersystem equals the sum of the energies of the subsystems.
- Like all perturbation-based methods, the SplitGAS method is not variational.

In the present paper we discussed a SplitGAS-CI implementation in which only the CI parameters are optimized. We are currently implementing an extension of the method that combines the optimization of both the CI coefficients and the orbitals.

We have employed SplitGAS to study several diatomic molecules, including the challenging case of Cr_2 for which we have obtained good agreement with experiments comparable to all the known best theoretical calculations. We have demonstrated that a correct potential curve for the ground-state of a challenging molecule like Cr_2 may be obtained using a double or triple-ζ basis set and limited many-electron expansions. We are currently investigating whether this also holds for other states of this molecule as well as other transition metal dimers and trimers.

■ ASSOCIATED CONTENT

Supporting Information

Absolute energies (in hartree) calculated at different levels of theory and different basis sets for the systems presented here. This material is available free of charge via the Internet at http://pubs.acs.org.

■ AUTHOR INFORMATION

Corresponding Author

*E-mail: glimanni@umn.edu (G.L.M.); gagliard@umn.edu (L.G.).

Author Contributions

As first author, G.L.M. led efforts to develop the formalism and implement it into code. As second author, D.M. contributed to theory, code development, and implementation. Senior author L.G. conceived and managed the research effort, and senior author J.O. developed and integrated code into a functional software platform. Author F.A. provided an early theoretical outline from which the present work developed. Authors L.G. and G.L.M. wrote the manuscript, and all authors subsequently provided comments leading to a final version. All authors have given approval to the final version of the manuscript.

Notes

The authors declare no competing financial interest.

■ ACKNOWLEDGMENTS

This material is based upon work supported by the National Science Foundation under grant number CHE-1212575. D.M. was supported primarily by the National Science Foundation through the University of Minnesota MRSEC under Award Number DMR-0819885.

■ REFERENCES

(1) Mills, D. P.; Moro, F.; McMaster, J.; van Slageren, J.; Lewis, W.; Blake, A. J.; Liddle, S. T. *Nat. Chem.* **2011**, *3*, 454.
(2) Christou, G.; Gatteschi, D.; Hendrickson, D. N.; Sessoli, R. *MRS Bull.* **2000**, *25*, 66.
(3) Pederson, M. R.; Khanna, S. N. *Phys. Rev. B* **1999**, *60*, 9566.
(4) Vigara, L.; Ertem, M. Z.; Planas, N.; Bozoglian, F.; Leidel, N.; Dau, H.; Haumann, M.; Gagliardi, L.; Cramer, C. J.; Llobet, A. *Chem. Sci.* **2012**, *3*, 2576.
(5) Bozoglian, F.; Romain, S.; Ertem, M. Z.; Todorova, T. K.; Sens, C.; Mola, J.; Rodriguez, M.; Romero, I.; Benet-Buchholz, J.; Fontrodona, X.; Cramer, C. J.; Gagliardi, L.; Llobet, A. *J. Am. Chem. Soc.* **2009**, *131*, 15176.
(6) Pantazis, D. A.; Orio, M.; Petrenko, T.; Zein, S.; Bill, E.; Lubitz, W.; Messinger, J.; Neese, F. *Chem.—Eur. J.* **2009**, *15*, 5108.
(7) Pantazis, D. A.; Orio, M.; Petrenko, T.; Zein, S.; Lubitz, W.; Messinger, J.; Neese, F. *Phys. Chem. Chem. Phys.* **2009**, *11*, 6788.
(8) Roos, B. O.; Taylor, P. R.; Siegbahn, P. E. M. *Chem. Phys.* **1980**, *48*, 157.
(9) Andersson, K.; Malmqvist, P.-Å.; Roos, B. O. *J. Chem. Phys.* **1992**, *96*, 1218.
(10) Roos, B. O.; Andersson, K. *Chem. Phys. Lett.* **1995**, *245*, 215.
(11) Forsberg, N.; Malmqvist, P.-Å. *Chem. Phys. Lett.* **1997**, *274*, 196.
(12) Ghigo, G.; Roos, B. O.; Malmqvist, P. A. *Chem. Phys. Lett.* **2004**, *396*, 142.
(13) Witek, H. A.; Choe, Y. K.; Finley, J. P.; Hirao, K. *J. Comput. Chem.* **2002**, *23*, 957.
(14) Finley, J.; Malmqvist, P. Å.; Roos, B. O.; Serrano-Andres, L. *Chem. Phys. Lett.* **1998**, *288*, 299.
(15) Aquilante, F.; Malmqvist, P. A.; Pedersen, T. B.; Ghosh, A.; Roos, B. O. *J. Chem. Theory Comput.* **2008**, *4*, 694.
(16) Aquilante, F.; Pedersen, T. B.; Lindh, R. *J. Chem. Phys.* **2007**, *126*, 11.
(17) Aquilante, F.; Pedersen, T. B.; Lindh, R.; Roos, B. O.; De Meras, A. S.; Koch, H. *J. Chem. Phys.* **2008**, *129*, 8.
(18) Aquilante, F.; De Vico, L.; Ferré, N.; Ghigo, G.; Malmqvist, P.-Å.; Pedersen, T.; Pitonak, M.; Reiher, M.; Roos, B. O.; Serrano-Andrés, L.; Urban, M.; Veryazov, V.; Lindh, R. *J. Comput. Chem.* **2010**, *31*, 224.
(19) Aquilante, F.; Todorova, T. K.; Gagliardi, L.; Pedersen, T. B.; Roos, B. *J. Chem. Phys.* **2009**, *131*, 7.
(20) Malmqvist, P. Å.; Pierloot, K.; Shahi, A. R. M.; Cramer, C. J.; Gagliardi, L. *J. Chem. Phys.* **2008**, *128*, 204109.
(21) Huber, S. M.; Moughal Shahi, A. R.; Aquilante, F.; Cramer, C. J.; Gagliardi, L. *J. Chem. Theory Comput.* **2009**, *5*, 2967.
(22) Moughal Shahi, A. R.; Cramer, C. J.; Gagliardi, L. *Phys. Chem. Chem. Phys.* **2009**, *11*, 10964.
(23) Sauri, V.; Serrano-Andrés, L.; Moughal Shahi, A. R.; Gagliardi, L.; Vancoillie, S.; Pierloot, K. *J. Chem. Theory Comput.* **2011**, *7*, 153.
(24) Ma, D.; Li Manni, G.; Gagliardi, L. *J. Chem. Phys.* **2011**, *135*, 044128.
(25) Marti, K. H.; Ondik, I. M.; Moritz, G.; Reiher, M. *J. Chem. Phys.* **2008**, *128*, 014104.
(26) Neuscamman, E.; Yanai, T.; Chan, G. K. L. *J. Chem. Phys.* **2009**, *130*, 124102.
(27) Yanai, T.; Kurashige, Y.; Ghosh, D.; Chan, G. K. L. *Int. J. Quantum Chem.* **2009**, *109*, 2178.
(28) Ghosh, D.; Hachmann, J.; Yanai, T.; Chan, G. K. L. *J. Chem. Phys.* **2008**, 128.
(29) Kurashige, Y.; Yanai, T. *J. Chem. Phys.* **2011**, 135.
(30) Li Manni, G.; Aquilante, F.; Gagliardi, L. *J. Chem. Phys.* **2011**, *134*, 034114.
(31) Lowdin, P. O. *J. Chem. Phys.* **1951**, *19*, 1396.
(32) Nitzsche, L. E.; Davidson, E. R. *J. Chem. Phys.* **1978**, *68*, 3103.
(33) Staroverov, V. N.; Davidson, E. R. *Chem. Phys. Lett.* **1998**, *296*, 435.
(34) Shavitt, I. *Chem. Phys. Lett.* **1992**, *192*, 135.
(35) Papp, P.; Mach, P.; Hubac, I.; Wilson, S. *Int. J. Quantum Chem.* **2007**, *107*, 2622.

(36) Hubac, I.; Mach, P.; Papp, P.; Wilson, S. *Mol. Phys.* **2004**, *102*, 701.
(37) Mazziotti, D. A. *Chem. Rev.* **2012**, *112*, 244.
(38) Olsen, J.; Jorgensen, P.; Simons, J. *Chem. Phys. Lett.* **1990**, *169*, 463.
(39) Dunning, T. H. *J. Chem. Phys.* **1989**, *90*, 1007.
(40) Huber, K. P.; Herzberg, G. *Constants of Diatomic Molecules*; Van Nostrand Reinhold: New York, 1979.
(41) Coxon, J. A.; Hajigeorgiou, P. G. *J. Mol. Spectrosc.* **1990**, *142*, 254.
(42) Lofthus, A.; Krupenie, P. H. *J. Phys. Chem. Ref. Data* **1977**, *6*, 113.
(43) Bondybey, V. E.; English, J. H. *Chem. Phys. Lett.* **1983**, *94*, 443.
(44) Casey, S. M.; Leopold, D. G. *J. Phys. Chem.* **1993**, *97*, 816.
(45) Roos, B. O.; Lindh, R.; Malmqvist, P. A.; Veryazov, V.; Widmark, P. O. *J. Phys. Chem. A* **2005**, *109*, 6575.
(46) Douglas, N.; Kroll, N. M. *Annu. Phys.* **1974**, *82*, 89.
(47) Hess, B. A. *Phys. Rev. A* **1986**, *33*, 3742.
(48) Roos, B. O. *Collect. Czech. Chem. Commun.* **2003**, *68*, 265.
(49) Brynda, M.; Gagliardi, L.; Roos, B. O. *Chem. Phys. Lett.* **2009**, *471*, 1.
(50) Brynda, M.; Gagliardi, L.; Widmark, P. O.; Power, P. P.; Roos, B. O. *Angew. Chem., Int. Ed.* **2006**, *45*, 3804.
(51) La Macchia, G.; Li Manni, G.; Todorova, T. K.; Brynda, M.; Aquilante, F.; Roos, B. O.; Gagliardi, L. *Inorg. Chem.* **2010**, *49*, 5216.
(52) Ruiperez, F.; Aquilante, F.; Ugalde, J. M.; Infante, I. *J. Chem. Theory Comput.* **2011**, *7*, 1640.
(53) Andersson, K.; Roos, B. O.; Malmqvist, P. A.; Widmark, P. O. *Chem. Phys. Lett.* **1994**, *230*, 391.